# Grafting of oligoaniline on CdSe nanocrystals: spectroscopic, electrochemical and spectroelectrochemical properties of the resulting organic/inorganic hybrid

**Claudia Querner,[a] Peter Reiss,*[a] Malgorzata Zagorska,[b] Olivier Renault,[c] Renaud Payerne,[a] Françoise Genoud,[a] Patrice Rannou[a] and Adam Pron*[a]**

***Received 26th August 2004, Accepted 7th October 2004***
***First published as an Advance Article on the web 18th November 2004***
**DOI: 10.1039/b413183e**

We have synthesised a new organic/inorganic hybrid, in which electroactive aniline tetramer is grafted on the surface of quasi-monodispersed CdSe nanocrystals. The grafting reaction consists of two steps. First initial nanocrystal surface ligands (TOPO) are exchanged for 4-formyldithiobenzoate linker ligands, which contain an anchor function (the dithioate group) and an aniline grafting function (the aldehyde group). The condensation reaction between the primary amine group of aniline tetramer and the aldehyde group of the linker ligand results in the grafting of the former with simultaneous formation of an azomethine linkage between both reagents. The grafting reaction is nearly quantitative as demonstrated by $^1$H NMR, FTIR and XPS studies. Voltammetric, UV-visible and EPR spectroelectrochemical studies of the hybrid compound show that after the grafting process the polyconjugated molecule retains its electrochemical activity *i.e.* electrochemical switching between the completely reduced state (leucoemeraldine), the semi-oxidised state (emeraldine) and the completely oxidised state (pernigraniline) is possible.

## Introduction

Conjugated polymers have been extensively studied for almost three decades for two principal reasons. First, in their neutral (undoped) state they are semiconductors and can serve as active components of so-called "polymer electronics".[1] Second, using an appropriate doping reaction, which can be either of redox or acid–base nature, semiconducting conjugated polymers can be transformed into so-called "organic metals" which, among others, can be used as electrodes in organic electronic components and devices.[2]

Another aspect of "electroactive polymers science" should also be pointed out. Since recent generations of conjugated polymers are solution processable, they can easily be mixed with inorganic semiconductors or conductors to give new hybrid-type materials whose properties can be altered by the appropriate selection of the organic and inorganic components of the blend. Instructive examples of this approach have been reported by Huynh *et al.*[3] and more recently by Beek *et al.*,[4] Liu *et al.*[5] and Pientka *et al.*[6] They demonstrated that the use of a composite of an electron-donating organic polymer (poly(thiophene) derivatives or poly(*p*-phenylenevinylene) derivatives) with electron-accepting CdSe or ZnO nanocrystals in hybrid-type photovoltaic cells facilitates exciton dissociation and charge separation.

Blending of inorganic nanocrystals with conjugated polymers is an interesting and convenient method for the preparation of new materials with improved properties. However, the possibility of preparing true molecular hybrids, in which the polymer (oligomer) is attached to a nanocrystal *via* a covalent bond, seems even more tempting. Two principal types of such hybrids can be envisioned. In the first type inorganic nanoparticles are grafted on individual macromolecules of conjugated polymers *via* an appropriate spacer. Alternatively, in hybrids of the second type, conjugated oligomers or polymers are grafted on the functionalised nanocrystal surface.[7] A(II)B(VI) nanocrystals are especially well suited for the preparation of the latter type of hybrids because of a rather facile functionalisation of the nanocrystal surface. In this case, bi-functional nanocrystal ligands must be used, which contain an anchor group for the nanocrystal surface and a second functional group used for polymer (oligomer) grafting *via* an appropriate chemical reaction with its end or lateral group.

In this paper, we report on basic spectroscopic and electrochemical properties of the first CdSe nanocrystal/oligoaniline hybrid. To the best of our knowledge no semiconductor nanocrystal/poly- or oligoaniline hybrids have ever been prepared. For grafting on nanocrystals we have selected aniline tetramer in the oxidation state of emeraldine because it mimics to a large extent the behaviour of poly(aniline)—one of the most extensively studied conducting polymers. In particular, poly(aniline) shows interesting non-linear electrical transport properties in its undoped state[8] and can be easily transformed into an organic conductor *via* protonation with non-oxidizing acids[9] *i.e.* in the chemical environment where semiconductor nanocrystals remain intact. Thus by grafting of aniline tetramer on CdSe nanocrystals two types of molecular junctions can easily be obtained:

---

*preiss@cea.fr (Peter Reiss)
pron@cea.fr (Adam Pron)

semiconductor–semiconductor for the base form of the oligomer and semiconductor–conductor for its protonated form.

## Experimental

### Chemicals

Anhydrous solvents and reagents (Aldrich) were of the highest purity available. Trioctylphosphine (TOP, 90%) and hexadecylamine (HDA, 90%) were additionally purified by distillation.

### Preparation procedures

**CdSe nanocrystals preparation.** CdSe nanocrystals were prepared following the procedure described in detail in ref. 10. A mixed solvent consisting of 70% of hexadecylamine (HDA) and 30% of trioctylphosphine oxide (TOPO) was used as the reaction medium. The basic spectroscopic properties of the obtained TOPO-capped CdSe nanocrystals are summarised below:

$^1$H NMR ($CDCl_3$, 200 MHz): $\delta$ 1.7–1.4 (s, 6H), 1.19 (s, 36H), 0.81 (s, 9H). UV-vis ($CHCl_3$): $\lambda$ = 561 nm (excitonic peak), 460 nm (higher excited state).

**Synthesis of 4-formyldithiobenzoic acid (3).** 4-Formyldithiobenzoic acid was prepared from 4-bromobenzaldehyde in a three step procedure, consisting of aldehyde protection,[11] followed by a Grignard reaction to introduce the carbodithioate group[12] and finally aldehyde deprotection,[13] as shown in Scheme 1, with an overall yield of 45%.

Characterisation of the final product, **3′**: $^1$H NMR ($d_6$-acetone, 200 MHz): $\delta$ 10.03 (1H, s), 8.32 (2H, d, $J$ = 8.6 Hz), 7.72 (2H, d, $J$ = 8.6 Hz). $^{13}$C NMR ($d_6$-acetone, 200 MHz): $\delta$ 128.76 (2C), 129.71 (2C), 137.34, 193.75, 252.80. Elemental analysis calculated for $C_8H_5OS_2Na$: C, 47.05; H, 2.47; Na, 11.26; O, 7.83; S, 31.40. Found: C, 47.17; H, 2.65; S, 30.67%.

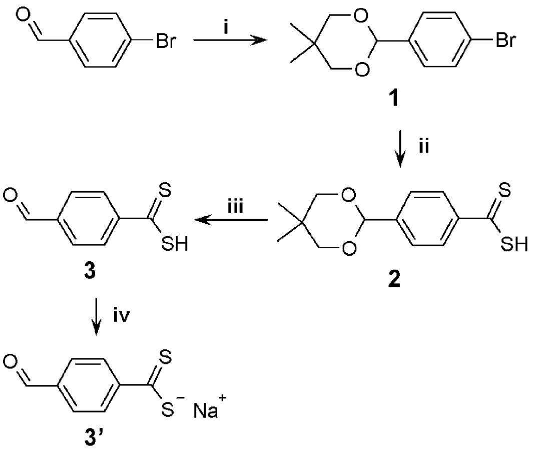

**Scheme 1** Synthetic pathway to obtain the bifunctional ligand **3**. *Reagents and conditions*: i) neopentyl glycol, $CF_3COOH$, toluene, 90 °C, 15 h; 94% yield; ii) Mg, THF, 60 °C, 2 h; $CS_2$, THF, 0 °C; 15 h; HCl; 62% yield; iii) $CHCl_3 : H_2O : CF_3COOH$ (2 : 1 : 10), 25 °C, 15 h; iv) $NaHCO_3$, 25 °C; 78% yield.

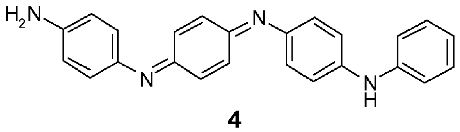

**4**

**Chart 1** Aniline tetramer (**4**).

**Preparation of aniline tetramer in the oxidation state of emeraldine (4).** Aniline tetramer (Chart 1) was prepared *via* oxidative coupling of *N*-phenyl-1,4-phenylenediamine ($C_{12}H_{12}N_2{\cdot}HCl$) as described in ref. 14.

$^1$H NMR ($d_6$-DMSO, 200 MHz): $\delta$ 8.37 (1H, s, N–*H*), 7.23 (2H, d, $J$ = 7 Hz), 7.11 (4H, d, $J$ = 5 Hz), 7.0–6.7 (9H, m), 6.62 (2H, d, $J$ = 8 Hz), 5.51 (2H, s, N–$H_2$). UV-vis (DMSO): $\lambda_{max}$ = 306 nm, $\lambda$ = 591 nm. IR ($\nu$/cm$^{-1}$): 1597 (s), 1497 (s), 1320 (m), 1166 (w), 839 (m), 745 (m), 692 (w).

**Ligand exchange and aniline tetramer grafting.** The ligand exchange–aniline tetramer grafting sequence is schematically presented in Scheme 2.

Step i: Bifunctional ligand **3′** (12 mg, 0.06 mmol) is dissolved in 10 mL of ethanol under inert atmosphere, then CdSe nanocrystals (10 mg) in 10 mL of chloroform are added and the mixture is stirred for 2 h at room temperature which is sufficient for essentially quantitative exchange of TOPO for **3′**. In the subsequent text nanocrystals containing 4-formyldithiobenzoate surface ligands will be termed **CdSe-3′**.

Step ii: A solution of aniline tetramer (**4**) (50 mg, 0.137 mmol) in 10 mL ethanol is added dropwise to the solution of aldehyde functionalised nanocrystals **CdSe-3′**. The mixture is then refluxed overnight under inert atmosphere. The formed black precipitate is filtered under inert atmosphere and washed repeatedly first with methanol, in order to extract

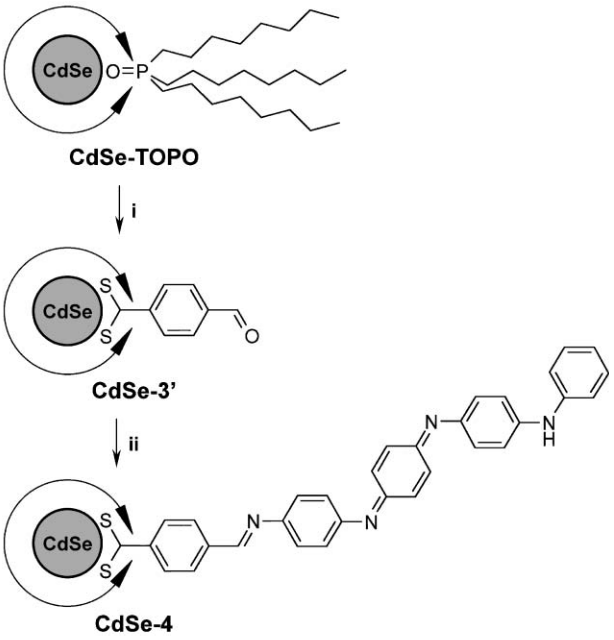

**Scheme 2** Grafting sequence of aniline tetramer (**4**) on CdSe nanocrystals *via* the bifunctional ligand **3′**. *Reagents and conditions*: i) **3′**, EtOH–$CHCl_3$, rt, 2 h; ii) **4**, EtOH, 80 °C, 15 h; 64% yield.

non-reacted tetramer, then with chloroform, with the goal to remove non-grafted aldehyde ligand. The final black solid, consisting of CdSe nanocrystals with aniline tetramer grafted on their surface *via* the bridging ligand, is abbreviated in the subsequent text as **CdSe-4** (7 mg, 64% yield).

Characterisation of the product **CdSe-4**: $^1$H NMR ($d_6$-DMSO, 200 MHz): $\delta$ 7.99 (6H, s), 7.2–6.6 (17H, m). UV-vis (DMSO): $\lambda_{max}$ = 325 nm, $\lambda$ = 618 nm. IR ($\nu$/cm$^{-1}$): 1697 (w), 1597 (s), 1504 (vs), 1297 (s), 1166 (m), 1012 (w) (Ar–$CS_2^-$), 819 (m), 750 (m), 696 (w).

**Synthesis of model compound (5).** For comparative reasons we have synthesised a model compound (**5**), shown in Chart 2, which is identical to the organic part of **CdSe-4**, apart from its terminal bromine group. Its preparation procedure can be briefly described as follows. A solution of aniline tetramer (**4**) (366 mg, 1 mmol) in 20 mL of anhydrous ethanol is added dropwise to the solution of *p*-bromobenzaldehyde (185 mg, 1 mmol) in 10 mL of the same solvent and the mixture is heated overnight under reflux. The resulting precipitate is filtered under inert atmosphere and washed with a large excess of methanol, chloroform and then dried in vacuum to give a black solid (405 mg, 74% yield).

$^1$H NMR ($d_6$-DMSO, 200 MHz): $\delta$ 8.43 (1H, s), 8.11 (5H, s), 7.8–7.4 (3H, m), 7.2–6.6 (14H, m). UV-vis (DMSO): $\lambda_{max}$ = 325 nm, $\lambda$ = 618 nm.

### Characterisation techniques

The synthesised products were identified by $^1$H and $^{13}$C NMR on a Bruker AC 200 MHz spectrometer (using deuterated solvents as specified, according to the solubility of the material, containing TMS as internal standard), as well as by elemental analysis, carried out by the Analytical Service of CNRS Vernaison (France). FT-IR spectra were recorded on a Perkin-Elmer paragon500 spectrometer (wavenumber range: 4000–400 cm$^{-1}$; resolution 2 cm$^{-1}$) using the ATR technique. Solution UV-vis spectra were recorded on a HP 8452A spectrometer (wavelength range 190–820 nm). Powder X-ray spectra were obtained with a Philips X'Pert MPD diffractometer using a Co X-ray source operated at 50 kV and 35 mA with a secondary graphite monochromator. AFM measurements were performed with a Nanoscope IIIa (Digital Instruments).

**XPS spectroscopy.** XPS measurements were performed under ultra-high vacuum conditions (base pressure in the analysis chamber: $5 \times 10^{-9}$ mbar) using an S-Probe spectrometer from Surface Science Instruments equipped with a monochromated, micro-focused Al $K_\alpha$ source ($h\nu$ = 1486.6 eV, spot size 150 × 800 μm) and a concentric hemispherical analyser.

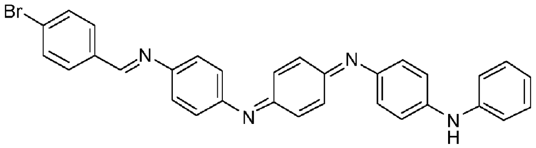

**5**

**Chart 2** Model compound (**5**).

High-resolution spectra were acquired with steps of 30 meV at a pass energy of 50 eV. The overall energy resolution of the measurements (analyser and X-ray line width combined) was thus 0.8 eV. Elemental quantification was performed by the analysis of the integral intensity of each core-level line weighed by its corresponding Scofield sensitivity factor available from the internal database of the acquisition software. Deconvolution of the core-level peak profiles was performed by using a Shirley background subtraction and peaks of mixed Gaussian–Lorentzian shape.

**Cyclic voltammetry.** Cyclic voltammetry investigations were carried out in a one-compartment electrochemical cell using a platinum counter electrode, an Ag/0.1 M $AgNO_3$ reference electrode and as the electrolyte a 0.1 M $Bu_4NBF_4$ solution in acetonitrile (1.646 g in 50 mL) to which 0.02 mol (250 mg) of diphenyl phosphate was added. Thin films of **CdSe-4**, **4** and **5** were deposited by casting from DMSO solutions on a Pt working electrode of 5 mm$^2$ surface area. The reference electrode was calibrated *vs.* the ferrocene redox couple measured in the same conditions.

**UV-vis spectroelectrochemistry.** In spectroelectrochemical experiments the same electrolytic solution, counter and reference electrodes were used as in the case of cyclic voltammetry investigations. Thin layers of **CdSe-4** and **5** were deposited on an ITO working electrode by casting from DMSO solution. The UV-vis-NIR spectra were measured on a Perkin Elmer Lambda 2 spectrometer (wavelength range 280–1100 nm).

**EPR spectroelectrochemistry.** EPR spectroelectrochemical experiments were carried out using an ER X-band Bruker spectrometer. The spectroelectrochemical cell consisted of an EPR tube to which three wire-type electrodes were inserted. The working electrode consisted of a Pt wire with a thin film of **CdSe-4** or **5** deposited on it. Another Pt wire was used as the counter electrode whereas an Ag wire served as pseudo-reference. The potential of the pseudo-reference electrode measured *vs.* 0.1 M $AgNO_3$ was 336 mV. The spin response to the applied electrode potential was measured in both increasing and decreasing potential modes in the same electrolyte as those used for cyclic voltammetry and UV-vis spectroelectrochemistry, using 20 mV increments. For each experimental point the EPR susceptibility was determined by double integration of the EPR signal.

## Results and discussion

### Basic spectroscopic and structural properties of the hybrid CdSe-4

An important feature of the newly developed bi-functional ligand, sodium 4-formyldithiobenzoate (**3′**), is its ability to efficiently exchange the initial TOPO ligands on the CdSe surface under mild conditions. As judged from $^1$H NMR spectroscopy and more precisely from the decrease of intensity of the signal originating from the aliphatic protons of TOPO, a

1 h room temperature reaction is sufficient to quasi-quantitatively (>95%) exchange the initial ligands with **3′**. This reaction is carried out in chloroform, which is a co-solvent for TOPO functionalised CdSe nanocrystals as well as for free TOPO, and an approximately 10-fold excess of the carbodithioate ligand with respect to the calculated molar quantity of surface TOPO molecules is used. The resulting compound **CdSe-3′** can then be conveniently transformed into **CdSe-4** *via* a simple condensation reaction between the aldehyde group of the carbodithioate surface ligand and the primary amine group of aniline tetramer. The formation of **CdSe-4** is manifested by the disappearance of the $^1$H NMR peaks at 10 ppm and 5.5 ppm, which are characteristic of the reacting groups in both substrates *i.e.* the aldehyde proton of **3′** and the terminal amine proton of **4**, respectively. The spectrum of the organic/inorganic hybrid **CdSe-4** consists of two sets of broad, poorly resolved lines at *ca.* 8 ppm and in the range of 6.6 to 7.2 ppm (Fig. 1). The broadening is most probably caused by restricted motion of the tetraaniline grafted on the nanocrystal surface *via* the phenylene–azomethine linking group.[15] This can be additionally corroborated by the comparison of the spectra of **CdSe-4** and the model compound **5**. In both cases lines in the same spectral range are observed, consistent with their chemical constitution. The model compound, being a "free" molecule, gives a better resolved spectrum, which is however complicated by the coexistence of positional isomers together with *cis*–*trans* isomerism.

The IR spectra recorded for **CdSe-4** are in agreement with the $^1$H NMR data. In particular the peak at 1697 cm$^{-1}$ characteristic of the C=O stretchings in **CdSe-3′** disappears upon aniline tetramer grafting, which indicates that the grafting process is quantitative and consumes all aldehyde groups present on the nanocrystal surface. The dithioate anchor function gives rise to a weak band at 1012 cm$^{-1}$,[16] which is absent in the spectra of aniline tetramer (**4**) and the model compound **5**. Consistent with the grafting *via* the primary amine group, its characteristic band at 1380 cm$^{-1}$, present in the free tetramer spectrum, is absent in the spectrum of the hybrid.

Ligand exchange and tetramer grafting do not lead to the formation of extended aggregates of the functionalised nanocrystals. Fig. 2 shows an AFM image of the hybrid **CdSe-4**, after drop casting from a diluted DMSO solution onto a silica substrate. Mainly isolated particles and to a lesser extent aggregates comprising a small number of particles are visible. The mean size of the individual particles determined by height analysis (3.8 nm) is slightly bigger than the value based on the documented correlation between the size (from TEM) and the position of the exciton absorption peak in the UV-vis spectrum of the original TOPO-capped CdSe nanocrystals (3.3 nm).[17] We attribute this difference to the organic shell, consisting of the aniline tetramer and the linking ligand. Even though squeezed together by the AFM tip, it contributes to the overall size of the hybrid, whereas in TEM it is generally not visible.

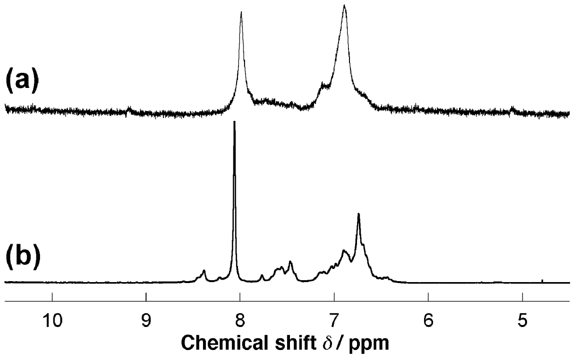

**Fig. 1** $^1$H NMR spectra of (a) the hybrid **CdSe-4**, and (b) the model compound (**5**).

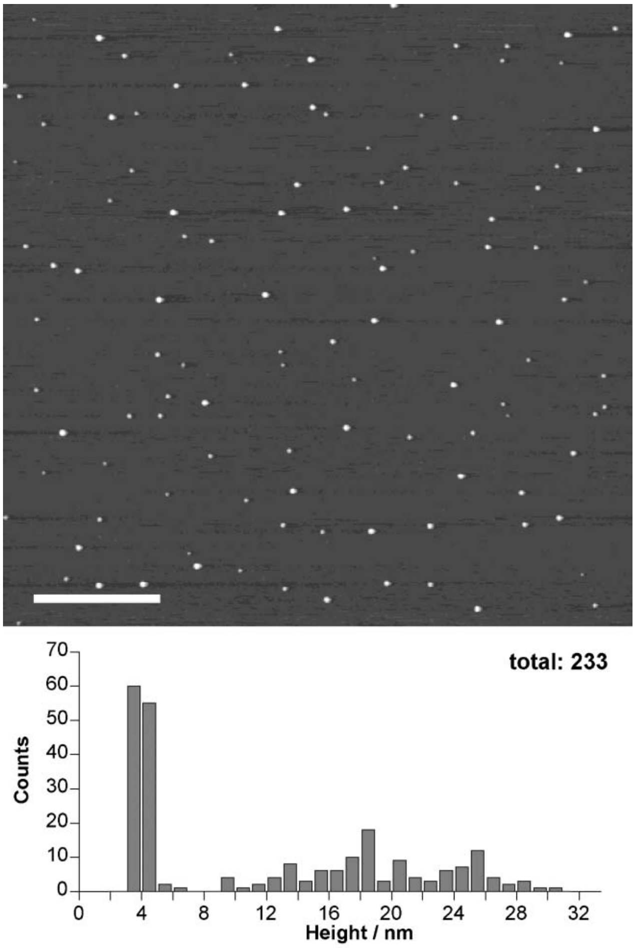

**Fig. 2** Top: AFM image (tapping mode) of the hybrid **CdSe-4** on a silica substrate (scale bar: 1 μm). Bottom: Height analysis.

Determination of the particle size by powder X-ray diffraction using the Scherrer formula leads to a value of *ca.* 4.5 nm. Due to the excessive broadening of the reflections, it is however difficult to determine the actual peak width, which explains the slight discrepancy with the AFM results. The diffractogram of **CdSe-4**, exhibiting the typical features of wurtzite CdSe nanocrystals,[18] is shown in Fig. 3.

In order to characterise the grafted oligomer–nanocrystal interface we have performed XPS studies of **CdSe-4**. In the analysis of the XPS data one must however be aware of the fact that the synthesised hybrid is a complex system, which in

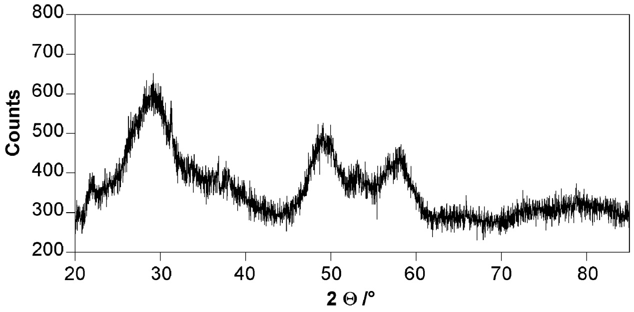

**Fig. 3** Powder X-ray diffraction spectrum of the hybrid **CdSe-4**.

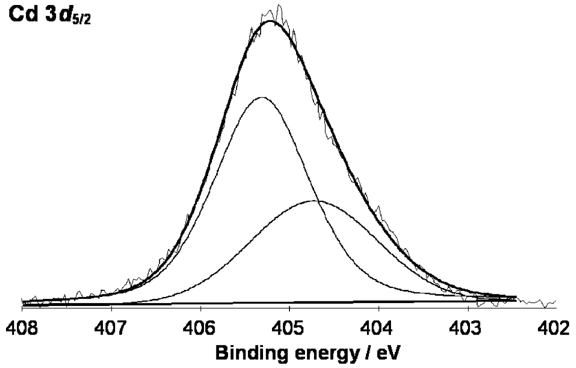

**Fig. 5** Detailed spectrum of the Cd $3d_{5/2}$ level of the hybrid **CdSe-4**.

the simplest approximation can be considered as consisting of the stoichiometric core of the nanocrystal, its strongly non-stoichiometic surface and a layer containing the grafted organic molecules. This makes quantitative determination difficult because for all elements determined the elastic mean free paths are smaller than the size of the object studied. This means that the intensity of a given photoemission should be proportional to the number of emitting atoms weighted by a specific attenuation factor. The latter cannot be easily calculated, especially in view of the presence of the organic layer of the grafted oligomers on the surface of the nanocrystal. In other words the determined contents of the elements constituting the organic part of the hybrid (C, N, S) and the inorganic one (Cd, Se) (in atom%) must be treated as apparent. Moreover, it is expected that the contents of the organic part elements should be overestimated taking into account that the grafted oligomers constitute the outer layer.

The XPS spectrum of **CdSe-4** deposited on the surface of a single crystal silicon substrate is shown in Fig. 4. The peaks corresponding to the photoemission from the core levels of all expected elements are clearly seen: the 3d peak of Cd at 405 eV close to the N 1s level at 399 eV, the 3d peak of Se at 54 eV, the 2p peak of S at 159 eV, the C 1s peak at 285 eV. In addition, a peak at 531 eV, attributed to O from the oxidised Si substrate, can be distinguished, along with the 2p and 2s peaks of Si around the S 2p peak; this reflects a non-continuous **CdSe-4** layer on Si.

Similarly as previously observed for TOPO-capped CdSe nanocrystals,[19] the surface layer of CdSe in the **CdSe-4** hybrid is strongly nonstoichiometric, showing a significant excess of cadmium atoms on the surface with the Cd to Se atomic ratio equal to 2.7. The Cd $3d_{5/2}$ spectral line (Fig. 5) can be deconvoluted into two components: the principal one at 405.3 eV whose binding energy is close to that measured for large size CdSe crystals, which probably corresponds to Cd atoms surrounded by saturated Se coordination spheres. The second one, at lower binding energy, should be attributed to those surface cadmium atoms which are complexed with the oligomer. This signal accounts for *ca.* 30% of the integrated total intensity.

Two XPS lines are especially interesting for the characterisation of the oligomer grafted on the nanocrystal surface, namely the S 2p and the N 1s peaks. The former should provide information concerning the chelating process since the anchor function contains two sulfur atoms, the latter is very useful in the determination of the oxidation state of the oligomer grafted on the CdSe surface. Unfortunately, the S 2p peak interferes with that originating from the Se $3p_{3/2}$ core emission, this makes any detailed analysis difficult. For this reason in the subsequent text we limit ourselves to the discussion of the N 1s spectrum (Fig. 6). In the simplest approach the observed broad peak can be deconvoluted into two components at 398.5 and 399.6 eV attributed to the amine and imine nitrogen atoms, respectively.[20] The organic part of the hybrid consists of the aniline tetramer attached to phenylene dithioate *via* an azomethine group (see Scheme 2 above). It is therefore not unexpected that the N 1s spectrum

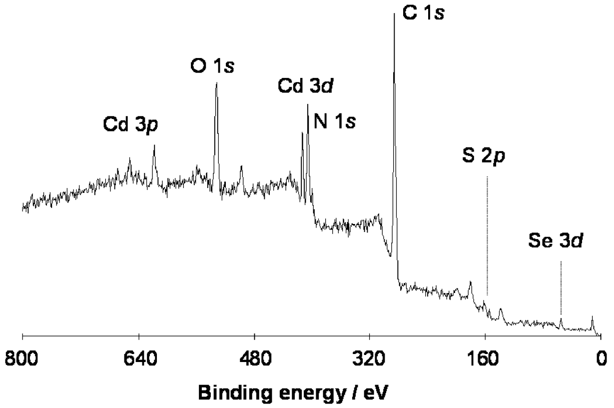

**Fig. 4** XPS survey spectrum of the hybrid **CdSe-4**.

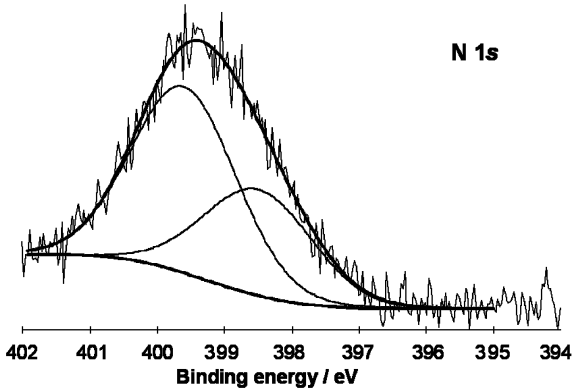

**Fig. 6** Detailed spectrum of the N 1s level of the hybrid **CdSe-4**.

of the hybrid resembles that of free aniline tetramer, not attached to the nanocrystal (see Chart 1), since in both compounds only amine and imine nitrogen co-exist.

Taking into account the complexity of **CdSe-4**, it is difficult to extract quantitative data from the XPS spectra, however they provide qualitative information of significant importance. In particular they show a clear feature of the grafting reaction which is manifested by the co-existence of two types of Cd atoms—complexed and non-complexed. Moreover, the comparison of the N 1s spectra of the free and the grafted tetramer indicates that, consistent with NMR data, the grafting process is a simple condensation reaction.

The chemical nature of the organic part of **CdSe-4**, consistent with Scheme 2, is also corroborated by UV-vis spectroscopy. It must be noted here that because of the high molar absorption coefficients the bands originating from the organic part of the hybrid dominate, rendering the bands originating from the nanocrystals essentially invisible. In the spectrum of the hybrid (Fig. 7), two bands can be distinguished at 325 nm and at 618 nm, both being characteristic of the base form of the grafted ligand. The higher energetic band is ascribed to the π–π* transition in the aromatic ring whereas the band at lower energy is attributed to an excitonic-type transition between the HOMO level of the quinone ring and the LUMO level of the benzene ring, respectively.[21] Thus, the presence of the band at 618 nm confirms that the grafted oligomer is in the semi-oxidised state of emeraldine, in which the benzene and quinone rings coexist. In polyconjugated systems the positions of the bands originating from electronic transitions involving π electrons are very sensitive to the conjugation length. For this reason the π–π* transition band and the excitonic band in **CdSe-4** are bathochromically shifted by 19 nm and 27 nm with respect to the positions of these bands in free aniline tetramer. This is a pure consequence of the fact that upon grafting the conjugation is extended to the linking molecule *via* the azomethine group (see Scheme 2).

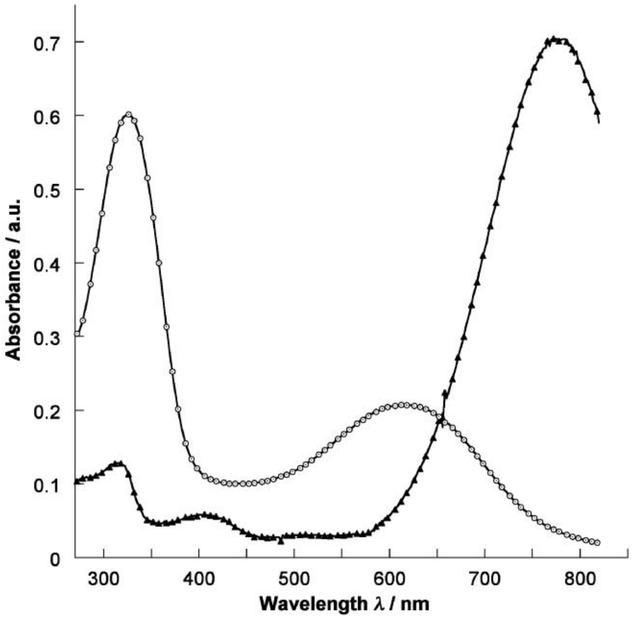

**Fig. 7** UV-visible absorption spectra of the hybrid **CdSe-4** in protonated form (filled up-triangles) and deprotonated form (hollow circles), registered in DMSO solutions.

Similarly to free aniline oligomers and polymers, the organic part of **CdSe-4** undergoes protonation if an appropriate protonating agent is added to its solution. The protonation is manifested by a total disappearance of the excitonic band at 618 nm and a significant decrease of the π–π* transition band intensity. Simultaneously two new bands attributed to the protonated state appear at *ca.* 405 nm and 780 nm, the former corresponding to the polaronic band–π* transition, the latter being characteristic of the localised polaron-type charge carriers.[22]

It is known that protonation of the semi-oxidised form of poly(aniline) or its oligomers leads, through charge redistribution, to a so-called "polaron lattice".[23] From the chemical point of view the created polarons are radical cations of the semi-quinone structure. For this reason it is convenient to study the protonation process by EPR spectroscopy. The analysis of the shape of the EPR signal may in this case provide important information concerning the mobility of charge carriers introduced into the system *via* protonation. However, such investigations have to be carried out with extreme care, since other than intrinsic properties of the material may influence the EPR linewidth. In particular the presence of even minute amounts of fixed paramagnetic centres, such as for example adsorbed oxygen molecules, significantly broadens the EPR line attributed to the mobile, spin carrying polarons.[24] Therefore any comparative study of charge mobility in aniline oligomers requires the use of vacuum line techniques and extended pumping until the EPR line parameters stabilise.

As expected neither **CdSe-4** nor **4** give any EPR signal in their semi-oxidised base forms. Protonation with 1 M HCl gives rise, in both cases, to clear EPR lines which are Lorentzian in shape and differ in their peak to peak width ($\Delta H_{pp}$) (Fig. 8). In particular, the protonated form of **4** is

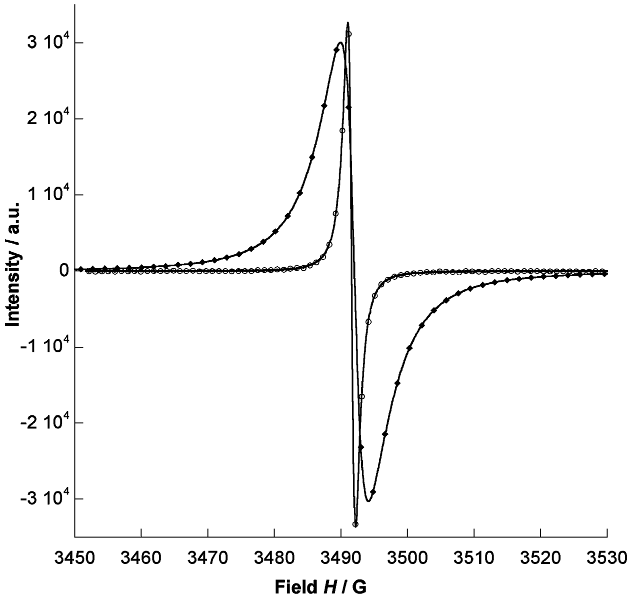

**Fig. 8** EPR signal of "free" aniline tetramer (**4**) (hollow circles) and hybrid **CdSe-4** (filled diamonds) protonated by 1 M HCl.

characterised by a narrow EPR line ($\Delta H_{pp}$ = 1.2 G) consistent with its rather high conductivity in the doped state.[25] The grafted ligand shows, after protonation, a significantly broader line ($\Delta H_{pp}$ = 4.2 G) indicating reduced charge mobility as compared to the case of the free tetramer. This is surprising because spectroscopic studies of the base forms of both systems seem to indicate a slightly more extended conjugation in **CdSe-4** as compared to **4**. However, the charge mobility as experienced by EPR spectroscopy is a microscopic property which principally depends on the conformation of the chain carrying the spin and its immediate vicinity. It can be therefore postulated that the grafting of the molecule on the nanocrystal surface induces, in its protonated state, unfavourable conformational changes as far as charge mobility properties are considered. Additionally, an increase in the local disorder impeding to some extent the intermolecule hopping may contribute to the line broadening.

This is only one of the possible explanations. The contribution of the spin–orbit coupling between the mobile organic parts of the hybrid and the nuclei constituting the nanocrystal cannot be excluded, especially in view of the conjugation extending essentially to the surface of the nanocrystal.

## Electrochemical and spectroelectrochemical properties of the hybrid CdSe-4

Aniline tetramer, similarly to poly(aniline), is electrochemically active. Its electrochemical switching from the completely reduced state through the semi-oxidised state to the completely oxidised state is possible by potential scanning. In the completely reduced state (leucoemeraldine state) all nitrogen atoms are of amine nature, 50% of them are transformed into the imine form during the first oxidation process to give the emeraldine oxidation state. The second oxidation process leads to the transformation of the remaining 50% of amine nitrogens into imine ones, resulting in the pernigraniline state.

We were tempted to verify to what extent the grafting of an electrochemically active ligand on the nanocrystal surface influences its electrochemical behaviour. For this reason, we have carried out comparative cyclic voltammetry (CV) and spectroelectrochemical studies of **CdSe-4** and **5**. Voltammetric investigations of poly(aniline) or its oligomers are usually carried out in aqueous acidic electrolytes.[26] Unfortunately the pernigraniline form of the polymer (oligomer) formed at higher potentials is not stable and in acidic conditions undergoes hydrolytic degradation.[27] This process lowers the electroactivity of the system and severely perturbs the reverse scan. For this reason, it is better to perform the CV investigations in non-aqueous electrolytes such as $Bu_4NBF_4$–acetonitrile. However, cycling of poly(aniline) or its oligomers in this electrolyte leads to a very poor electrochemical response unless a good source of protons is added to the electrolytic solution.[28] This is understandable since electrochemical oxidation or reduction processes involve an exchange of protons between the polymer (oligomer) deposited on the electrode and the electrolyte. This process is of course greatly facilitated in the presence of a good protonating agent such as diphenyl phosphate, selected in this research.

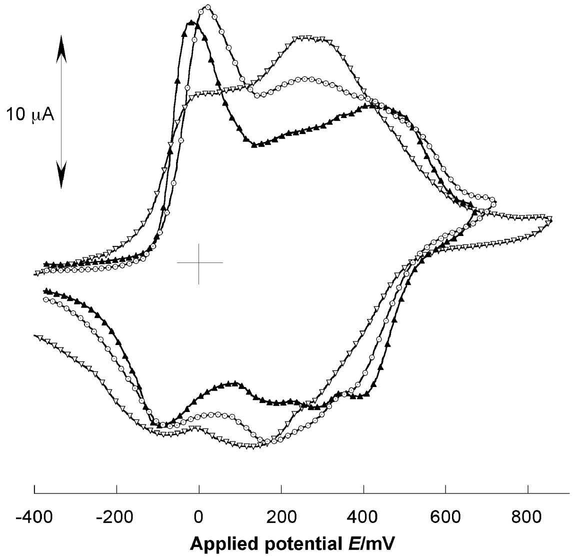

**Fig. 9** Cyclic voltammograms of thin films of aniline tetramer (**4**) (hollow down-triangles), model compound (**5**) (filled up-triangles) and the hybrid **CdSe-4** (hollow circles), registered in 0.1 M $Bu_4NBF_4$ solution in acetonitrile using $Ag/Ag^+$ as reference electrode and a scan rate of 25 mV $s^{-1}$.

Cyclic voltammograms of **4**, **CdSe-4** and **5** are shown in Fig. 9. For **5** the two redox couples discussed above—leucoemeraldine/emeraldine and emeraldine/pernigraniline—can clearly be distinguished. The former one gives rise to a relatively sharp anodic peak with a maximum at −15 mV and the corresponding cathodic peak at −90 mV. The second redox process is characterised by a broad anodic peak with its even broader cathodic counterpart consisting of at least three strongly overlapping peaks. The immediate effect associated with the grafting is a change in the slope of the first anodic peak. Although the oxidation of **CdSe-4** starts at the same potential as in the case of **5**, the maximum of the first anodic peak is slightly shifted towards higher potentials by 35 mV to 20 mV. The second anodic peak registered for **CdSe-4** is broad and poorly defined. In fact, the second oxidation process occurs at any potential in the potential range from 150 mV to 600 mV. Assuming the same oxidation mechanism in **CdSe-4** and **5** we must attribute the observed differences in their voltammetric behaviour to structural and/or morphological features. Monodispersed, π-conjugated molecules of **5** should more easily form ordered structures assuring a more isoenergetic environment for molecules being oxidised. This leads, in turn, to narrower anodic peaks. It should be noted here that the first oxidation process is accompanied by protonation of the imine nitrogens (acid–base doping) whereas the second process involves dedoping (deprotonation).[28] The doping/dedoping sequence of reactions introduces a significant disorder to the system which is manifested by consecutive broadening of the cathodic peaks. For the grafted ligand in **CdSe-4** the translational freedom is blocked and for this reason its capability of the formation of ordered structures with isoenergetic environments is severely limited. As a result both of its anodic peaks are broadened. Note that in its second redox process **CdSe-4** can be more easily oxidised as compared to **5**. In contrast, in the cathodic part it is more difficult to reduce.

Since optical properties of the chromophore groups present in **CdSe-4** and **5** are extremely sensitive to even small changes in their oxidation and protonation states, it is convenient to follow their anodic oxidation by spectroelectrochemistry. For both compounds the spectroelectrochemical investigations were carried out in the increasing potential mode *i.e.* the first spectrum was registered for the most reduced form of the compound studied and the consecutive spectra were recorded for potentials increasing in 100 mV increments. The spectroelectrochemical behaviour of **CdSe-4** and **5** is almost identical showing that grafting of the ligand on the nanocrystal surface does not influence, to a measurable extent, the mechanism of its electrochemical oxidation.

Consistent with the cyclic voltammogram, at potentials below the onset of the first anodic peak, both **CdSe-4** and **5** are in their most reduced base state. The dominant peak, corresponding to the π–π* transition in the aromatic ring of the ligand and the model compound being in the most reduced state, is hypsochromatically shifted by *ca.* 25 nm (from 325 to 300 nm) as compared to the corresponding peak in the semi-oxidised form of these compounds (compare Figs. 7 and 10). However, even at these negative potentials, spectroscopic signatures of very low intensity characteristic of the partially oxidised state can be distinguished. These are a small peak at 430 nm and two broader bands around 600 nm and 1000 nm. The existence of these residual bands can be rationalised either by the incomplete reduction of both compounds due to kinetic reasons or by the high reactivity of their reduced form which locally reacts with traces of oxygen in the electrolyte or any other source of a suitable oxidizing agent. At $E = 0$ mV both compounds are already partially oxidised. It must be noted that the oxidation of the completely reduced forms of **CdSe-4** and **5** is accompanied by the simultaneous protonation of the oxidised segments with the protonating agent (diphenyl phosphate) added to the electrolytic solution. As has already been mentioned, the protonated state is characterised by a decrease of intensity of the band originating from the π–π* transition, a simultaneous growth (and hypsochromic shift) of a narrow band around 420 nm and an increasing absorption tail extended towards the near infrared (NIR) spectral region if the doping induced charge carriers (polarons) are delocalised. In the case of poly(aniline), the origin of these spectral features has been explained in terms of protonation induced band structure modification.[22] The same reasoning can be applied here. It is interesting to compare the spectrum recorded at $E = 200$ mV (Fig. 10b) with that obtained after protonation of the base form of semi-oxidised **CdSe-4** (Fig. 7). Both exhibit features of the protonated emeraldine, however the former shows a NIR absorption tail characteristic of delocalised carriers whereas in the latter a NIR peak characteristic of localised carriers is observed. This is in perfect agreement with the analysis presented above and shows additionally that the removal of the solvent facilitates the delocalisation of polarons due to more planar conformation in the solid state.

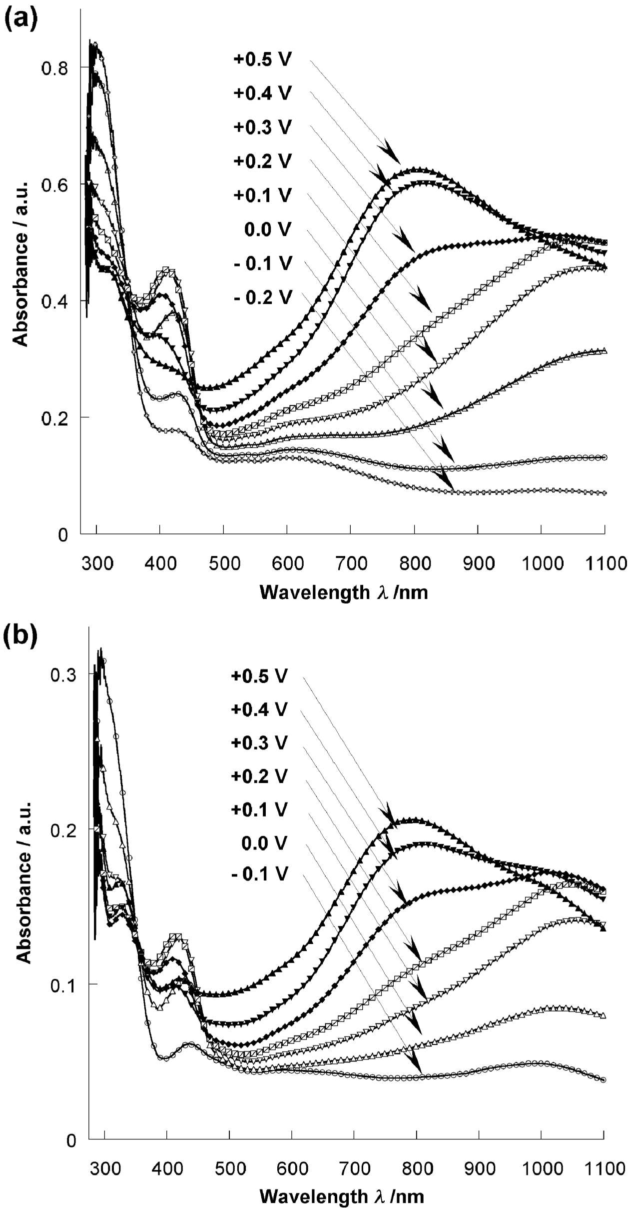

**Fig. 10** UV-vis-NIR spectra of (a) the model compound (**5**) and (b) the hybrid **CdSe-4** and registered for increasing electrode potential *E vs.* Ag/Ag$^+$, electrolyte: 0.1 M $Bu_4NBF_4$ solution in acetonitrile.

In further analysis of the spectroelectrochemical behaviour of both compounds it is convenient to distinguish two potentials ranges corresponding to two different redox processes; the first from −50 mV to 200 mV and the second from 200 mV to 500 mV. The first potential zone corresponds to the complete transformation of the most reduced forms **CdSe-4** and **5** into their fully protonated semi-oxidised forms. Thus with increasing potential the peak at 425 nm and the absorption tail extending to the NIR spectral region, which are characteristic of the semi-oxidised protonated state, grow in intensity. At the same time the intensity of the π–π* band decreases.

Spectral changes registered in the second potential zone are consistent with the oxidation of the protonated, semi-oxidised, forms of **CdSe-4** and **5** to the fully oxidised ones. This process is accompanied by deprotonation of the reaction product. First we note that above $E = 200$ mV the band at 415 nm, characteristic of the protonated state, starts to decrease. Second, a new band superimposed on the NIR absorption tail appears at *ca.* 800 nm and starts to dominate the spectrum at the highest potentials at the expense of the NIR absorption tail. Third, the band ascribed to the π–π* transition in the aromatic ring does not decrease any more but undergoes a bathochromic shift to *ca.* 320 nm. All these changes unequivocally indicate that the second oxidation results in increasing contents of deprotonated segments in the completely oxidised (pernigraniline) state. This, spectroelectrochemically observed, deprotonation (dedoping) accompanying the second redox process is also manifested in the cyclic voltammograms of **CdSe-4** and **5**. After the first redox process a high capacitance current is observed characteristic of the penetration of the dopant anions in the layers deposited on the electrode. After the second oxidation process this capacitance current strongly decreases indicating that both **CdSe-4** and **5** are present in their neutral base forms.

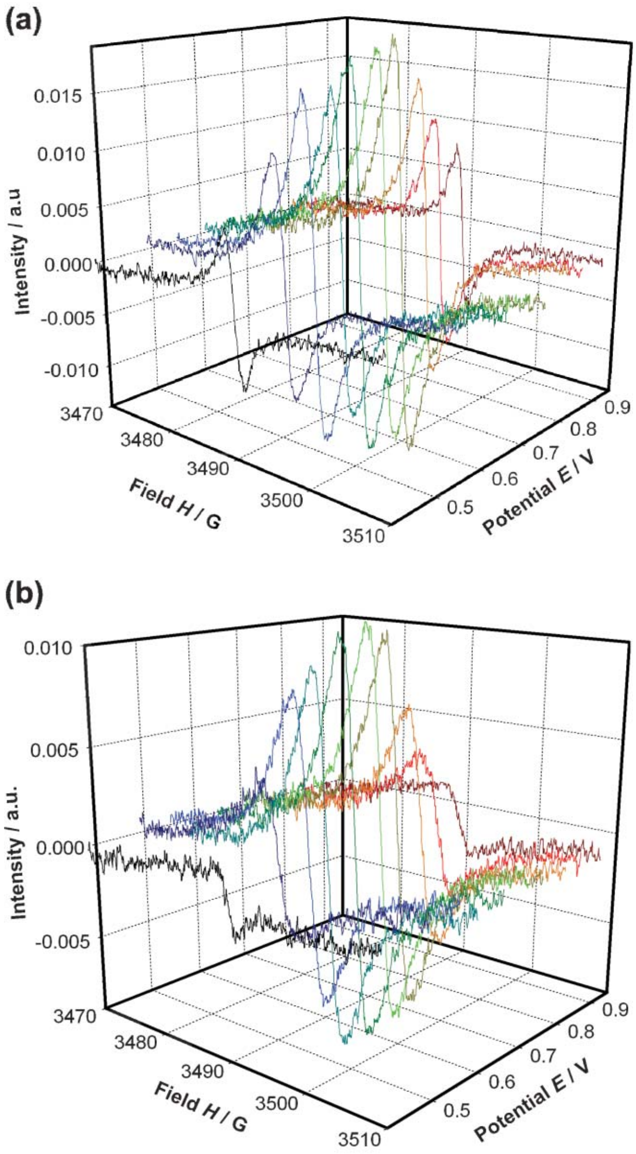

**Fig. 11** EPR signals for varying electrode potentials of (a) **CdSe-4** and (b) **5**, measured for increasing electrode potential *E vs.* Ag; electrolyte: 0.02 M diphenyl phosphate and 0.1 M $Bu_4NBF_4$ solution in acetonitrile.

Thus cyclic voltammetry studies combined with UV-vis spectroelectrochemistry clearly show that although the grafting of the ligand on the nanocrystal surface changes the shape of its voltammogram, its oxidation mechanism remains basically unchanged as compared to the case of the non-grafted model compound.

The similarity of the redox and protonation/deprotonation processes in **CdSe-4** and in oligoanilines can be additionally evidenced by EPR spectroelectrochemistry.

The evolution of the EPR signal with the increase of the electrode potential for **CdSe-4** and the model compound **5** is presented in Fig. 11. It should be noted here that the measured potential of the Ag pseudo-reference electrode used in the EPR spectroelectrochemical experiments *vs.* Ag/0.1 M $AgNO_3$ reference, used in other experiments, was 336 mV. This correction should be taken into account when comparing Figs. 9, 10 and 11. First, we notice that, in both cases, at potentials characteristic of the completely reduced state (0 mV *vs.* Ag) where the spinless base form of leucoemeraline is expected, a weak but measurable EPR signal, Lorentzian in shape, is observed. This signal originates from minute amounts of the non-reduced and protonated forms of **CdSe-4** and **5**, present on the electrode. This is consistent with the UV-vis spectroelectrochemical data (see Fig. 10) which also show the presence of minute amounts of the protonated semi-oxidised form of **CdSe-4** at the potentials below the onset of the first oxidation peak. With the increase of the electrode potential, the intensity of the EPR line increases, indicating an increasing amount of the semi-oxidised protonated form of **CdSe-4** on the electrode. The maximum of the EPR susceptibility is obtained for $E$ = 660 mV *vs.* Ag (324 mV *vs.* Ag/0.1 M $AgNO_3$), then the susceptibility starts to decrease indicating that further oxidation results in a growing content of the deprotonated (base) form of pernigraniline (Fig. 12). The

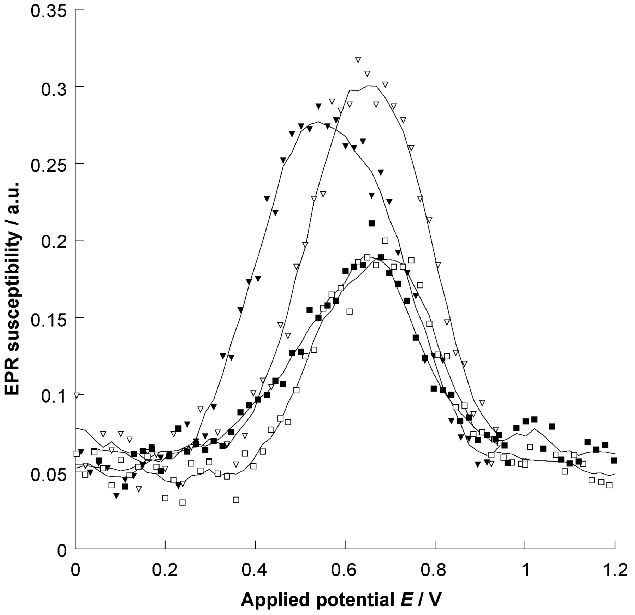

**Fig. 12** EPR susceptibility, obtained by double integration of the EPR signal for varying electrode potentials of **CdSe-4** (squares) and **5** (down-triangles) measured for increasing (hollow) and decreasing (filled) potential *E vs.* Ag; electrolyte: 0.02 M diphenyl phosphate and 0.1 M $Bu_4NBF_4$ solution in acetonitrile.

proposed sequence of oxidation reactions (spinless leucoemeraldine base–protonated, spin carrying emeraldine–spinless pernigraniline base) should lead to two oxidation peaks in cyclic voltammetry and one peak in the EPR spectroelectrochemical response, as observed experimentally. It should be also noted that the behaviour of **CdSe-4** is very reversible from the electrochemical standpoint since no hysteresis in the electrochemical spin response is observed for the reverse scan. In contrast, a clear hysteresis is observed for **5**, consistent with the cyclic voltammetry curves of both compounds studied (compare Figs. 9 and 12).

## Conclusions

To summarise, we have synthesised a new organic/inorganic hybrid consisting of oligoaniline molecules grafted on the surface of CdSe nanocrystals. The completeness of the grafting reaction was confirmed by $^1$H NMR, XPS and IR spectroscopies. The grafted polyconjugated ligand retains its electrochemical activity as proved by cyclic voltammetry and spectroelectrochemical UV-vis and EPR investigations. The developed grafting methods can easily be extended to other polyconjugated molecules or macromolecules and other semiconductor nanocrystals.

## Acknowledgements

The authors thank Dr. J. P. Travers for critical review of the manuscript and valuable discussions, and Dr. B. Divisia-Blohorn for help with cyclovoltammetric measurements.

**Claudia Querner,[a] Peter Reiss,*[a] Malgorzata Zagorska,[b]**
**Olivier Renault,[c] Renaud Payerne,[a] Françoise Genoud,[a] Patrice Rannou[a]**
**and Adam Pron*[a]**
*[a]Laboratoire de Physique des Métaux Synthétiques, UMR5819-SPrAM (CEA-CNRS-Univ. J. Fourier-Grenoble I), DRFMC, CEA-GRENOBLE, 17 rue des Martyrs, 38054 Grenoble cedex 9, France. E-mail: preiss@cea.fr; pron@cea.fr; Fax: +33 4 38 78 51 13*
*[b]Faculty of Chemistry, Warsaw University of Technology, Noakowskiego 3, 00-664 Warsaw, Poland*
*[c]SCPIO, DPTS, LETI, CEA-Grenoble, 17 rue des Martyrs, 38054 Grenoble cedex 9, France*

## References

1 (*a*) LED: S. R. Forrest, *Nature*, 2004, **428**, 911–918; A. Kraft, A. C. Grimsdale and A. B. Holmes, *Angew. Chem., Int. Ed.*, 1998, **37**, 4, 402–428; R. H. Friend, R. W. Gymer, A. B. Holmes, J. H. Burroughes, R. N. Marks, C. Taliani, D. D. C. Bradley, D. A. Dos Santos, J. L. Bredas, M. Logdlund and W. R. Salaneck, *Nature*, 1999, **397**, 121–128; (*b*) solar cells: G. Yu, J. Gao, J. C. Hummelen, F. Wudl and A. J. Heeger, *Science*, 1995, **270**, 1789–1791; M. Granström, K. Petritsch, A. C. Arias, A. Lux, M. R. Andersson and R. H. Friend, *Nature*, 1998, **395**, 257–260; C. J. Brabec, N. S. Sariciftci and J. C. Hummelen, *Adv. Funct. Mater.*, 2001, **11**, 1, 15–26; (*c*) FET: H. Sirringhaus, P. J. Brown, R. H. Friend, M. M. Nielsen, K. Bechgaard, B. M. W. Langeveld-Voss, A. J. H. Spiering, R. A. J. Janssen, E. W. Meijer, P. Herwig and D. M. de Leeuw, *Nature*, 1999, **401**, 685–688; C. D. Dimitrakopoulos and D. J. Mascaro, *IBM J. Res. Dev.*, 2001, **45**, 1, 11–27; H. E. Katz, Z. N. Bao and S. L. Gilat, *Acc. Chem. Res.*, 2001, **34**, 359–369; (*d*) LASER: N. Tessler, G. J. Denton and R. H. Friend, *Nature*, 1996, **382**, 695–697; F. Hide, M. A. DiazGarcia, B. J. Schwartz, M. R. Andersson, Q. B. Pei and A. J. Heeger, *Science*, 1996, **273**, 1833–1836; F. Hide, M. A. DiazGarcia, B. J. Schwartz and A. J. Heeger, *Acc. Chem. Res.*, 1997, **30**, 10, 430–436.

2 G. Gustafsson, Y. Cao, G. M. Treacy, F. Klavetter, N. Colaneri and A. J. Heeger, *Nature*, 1992, **357**, 477–479; C. J. Drury, C. M. J. Mutsaers, C. M. Hart, M. Matters and D. M. de Leeuw, *Appl. Phys. Lett.*, 1998, **73**, 1, 108–110; G. H. Gelinck, T. C. T. Geuns and D. M. de Leeuw, *Appl. Phys. Lett.*, 2000, **77**, 10, 1487–1489.

3 W. U. Huynh, J. J. Dittmer and A. P. Alivisatos, *Science*, 2002, **295**, 2425–2427.

4 W. J. E. Beek, M. M. Wienk and R. A. J. Janssen, *Adv. Mater.*, 2004, **16**, 12, 1009–1013.

5 J. Liu, T. Tanaka, K. Sivula, A. P. Alivisatos and J. M. J. Fréchet, *J. Am. Chem. Soc.*, 2004, **126**, 21, 6550–6551.

6 M. Pientka, V. Dyakonov, D. Meissner, A. Rogach, H. Weller, L. Lutsen and D. Vanderzande, *Nanotechnology*, 2004, **15**, 1, 163–170.

7 S. Roux, G. J. A. A. Soler-Illia, S. Demoustier-Champagne, P. Audebert and C. Sanchez, *Adv. Mater.*, 2003, **15**, 3, 217–221.

8 Y. Kieffel, J. P. Travers and D. Cottevieille, *Annu. Rep. Conf. Electr. Insul. Dielectr. Phenom.*, 2000, **1**, 52–56.

9 E. T. Kang, K. G. Neoh and K. L. Tan, *Progr. Polym. Sci.*, 1998, **23**, 2, 277–324.

10 P. Reiss, J. Bleuse and A. Pron, *Nano Lett.*, 2002, **2**, 7, 781–784.

11 C. Y. Zhang and J. M. Tour, *J. Am. Chem. Soc.*, 1999, **121**, 38, 8783–8790.

12 R. Colorado, R. Villazana and T. R. Lee, *Langmuir*, 1998, **14**, 22, 6337–6340.

13 H. Sashiwa, Y. Shigemasa and R. Roy, *Macromolecules*, 2000, **33**, 19, 6913–6915.

14 B. Dufour, P. Rannou, J. P. Travers, A. Pron, M. Zagorska, G. Korc, I. Kulszewicz-Bajer, S. Quillard and S. Lefrant, *Macromolecules*, 2002, **35**, 16, 6112–6120.

15 M. Kuno, J. K. Lee, B. O. Dabbousi, F. V. Mikulec and M. G. Bawendi, *J. Chem. Phys.*, 1997, **106**, 23, 9869–9882.

16 H. Gotthardt, W. Pflaumbaum and P. Gutowski, *Chem. Ber.*, 1988, **121**, 313–322; T. Gade, M. Streek and J. Voß, *Chem. Ber.*, 1988, **121**, 2245–2249.

17 W. W. Yu, L. Qu, W. Guo and X. Peng, *Chem. Mater.*, 2003, **15**, 14, 2854–2860.

18 C. B. Murray, D. J. Norris and M. G. Bawendi, *J. Am. Chem. Soc.*, 1993, **115**, 19, 8706–8715.

19 J. Taylor, T. Kippeny and S. J. Rosenthal, *J. Cluster Sci.*, 2001, **12**, 4, 571–582.

20 E. T. Kang, K. G. Neoh and K. L. Tan, *Adv. Polym. Sci.*, 1993, **106**, 135–190.

21 W. Zheng, M. Angelopulos, A. J. Epstein and A. J. MacDiarmid, *Macromolecules*, 1997, **30**, 24, 7634–7639.

22 Y. Xia, J. M. Wiesinger, A. G. MacDiarmid and A. J. Epstein, *Chem. Mater.*, 1995, **7**, 3, 443–445.

23 A. J. Epstein, J. M. Ginder, F. Zuo, R. W. Bigelow, H. S. Woo, D. B. Tanner, A. F. Richter, W. S. Huang and A. G. MacDiarmid, *Synth. Met.*, 1987, **18**, 1–3, 303–309.

24 E. Houze, M. Nechtschein and A. Pron, *Phys. Rev. B*, 1997, **56**, 19, 12263–12267.

25 R. Payerne, P. Rannou, D. Djurado, F. Genoud, A. Pron and J. P. Travers, *Synth. Met.*, 2004, submitted.

26 W.-S. Huang, B. D. Humphrey and A. G. MacDiarmid, *J. Chem. Soc., Faraday Trans. 1*, 1986, **82**, 8, 2385–2400.

27 A. Pron, F. Genoud, C. Menardo and M. Nechtschein, *Synth. Met.*, 1988, **24**, 3, 193–201.

28 M. Lapkowski, K. Berrada, S. Quillard, G. Louarn, S. Lefrant and A. Pron, *Macromolecules*, 1995, **28**, 4, 1233–1238.